

# **Long-term impacts of ocean wave-dependent roughness on global climate systems by coupled atmospheric global climate-wave model**

Tomoya SHIMURA • Nobuhito MORI • Tetsuya TAKEMI

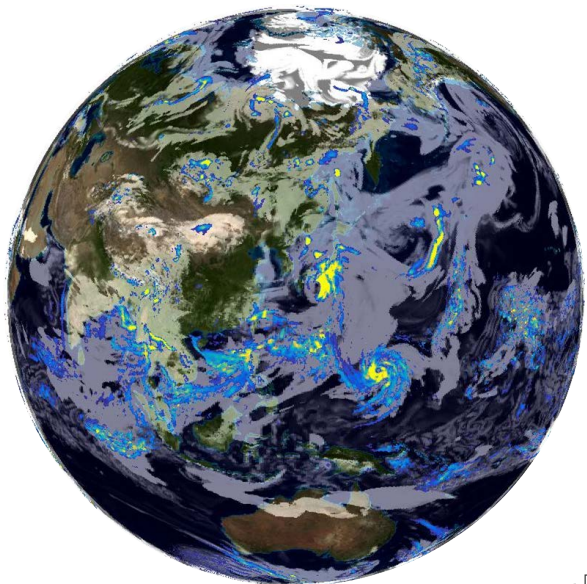
(Kyoto University, Japan)

Ryo MIZUTA

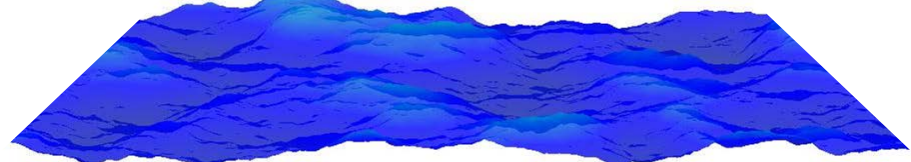
(Meteorological Research Institute, Japan)



# Atmospheric Global Climate Model MRI-AGCM

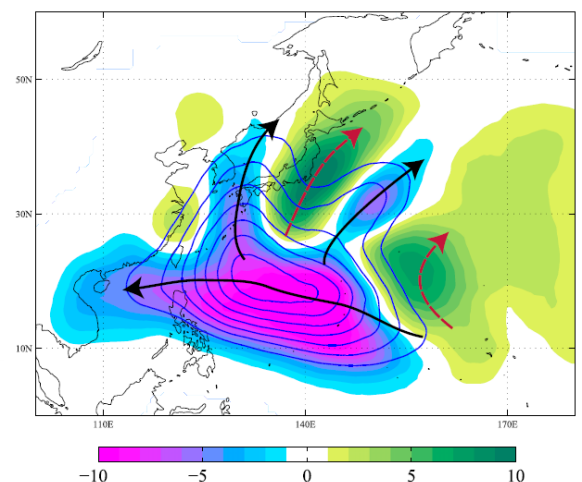
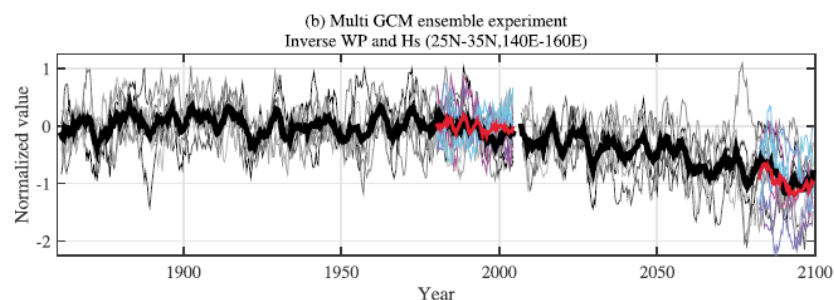
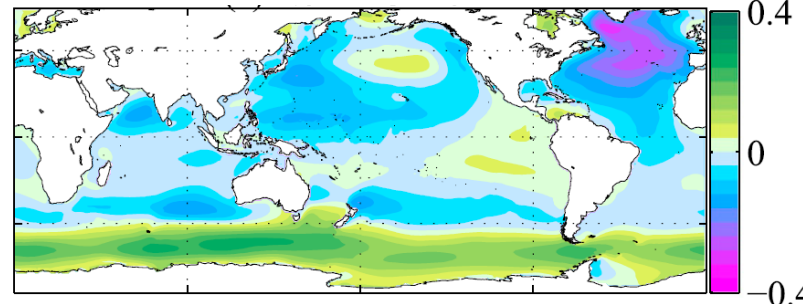


Wind ( $U_{10}$ )

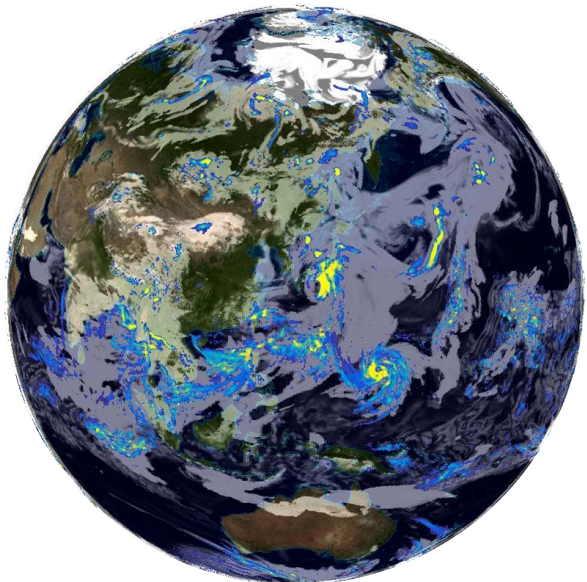


**WAVEWATCH III**

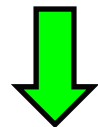
Climate change impacts on  
ocean wave climate  
(Mori et al. 2010, 2013;  
Shimura et al. 2015a, b, 2016a, b)



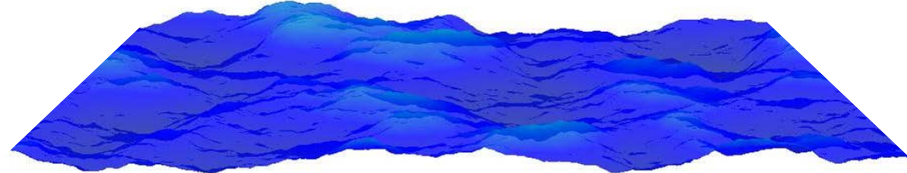
**Atmospheric Global  
Climate Model**  
**MRI-AGCM**



Wind ( $U_{10}$ )



Roughness length  
( $z_{0m}$ )



**WAVEWATCH III**

Bulk transfer relation

- Momentum

$$u_*^2 = C_m U^2$$

- Heat

$$\overline{w'\theta} = C_h |U| (\theta_a - \theta_g)$$

Previous studies

Weber et al., 1993

Janssen and Viterbo, 1996

Fan et al., 2012

Charles and Hemer, 2013

# Ocean Wave-Dependent Momentum Roughness Length

Wind speed dependent (Charnock relation)

$$z_0 = \alpha \frac{u_*^2}{g} \quad (\alpha: \text{Charnock parameter})$$

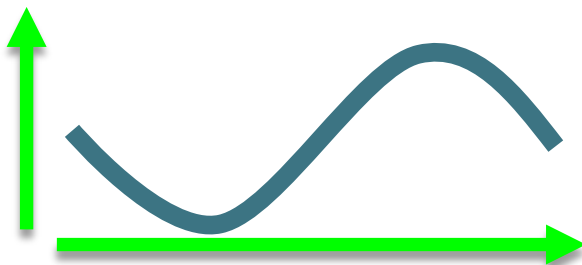
Wave steepness dependent

(Taylor and Yelland, 2001)

$$\frac{z_{0m}}{H_s} = A_1 \left( \frac{H_s}{L_p} \right)^{B_1}$$

$H_s$ : Significant wave height

$L_p$ : Peak wave length



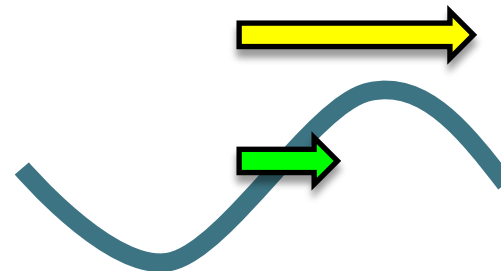
Wave age dependent

(Drennan et al., 2003)

$$\frac{z_{0m}}{H_s} = A_2 \left( \frac{u_*}{c_p} \right)^{B_2}$$

$H_s$ : Significant wave height

$C_p$ : Wind-sea peak wave phase speed



# Example of wave-coupled simulation

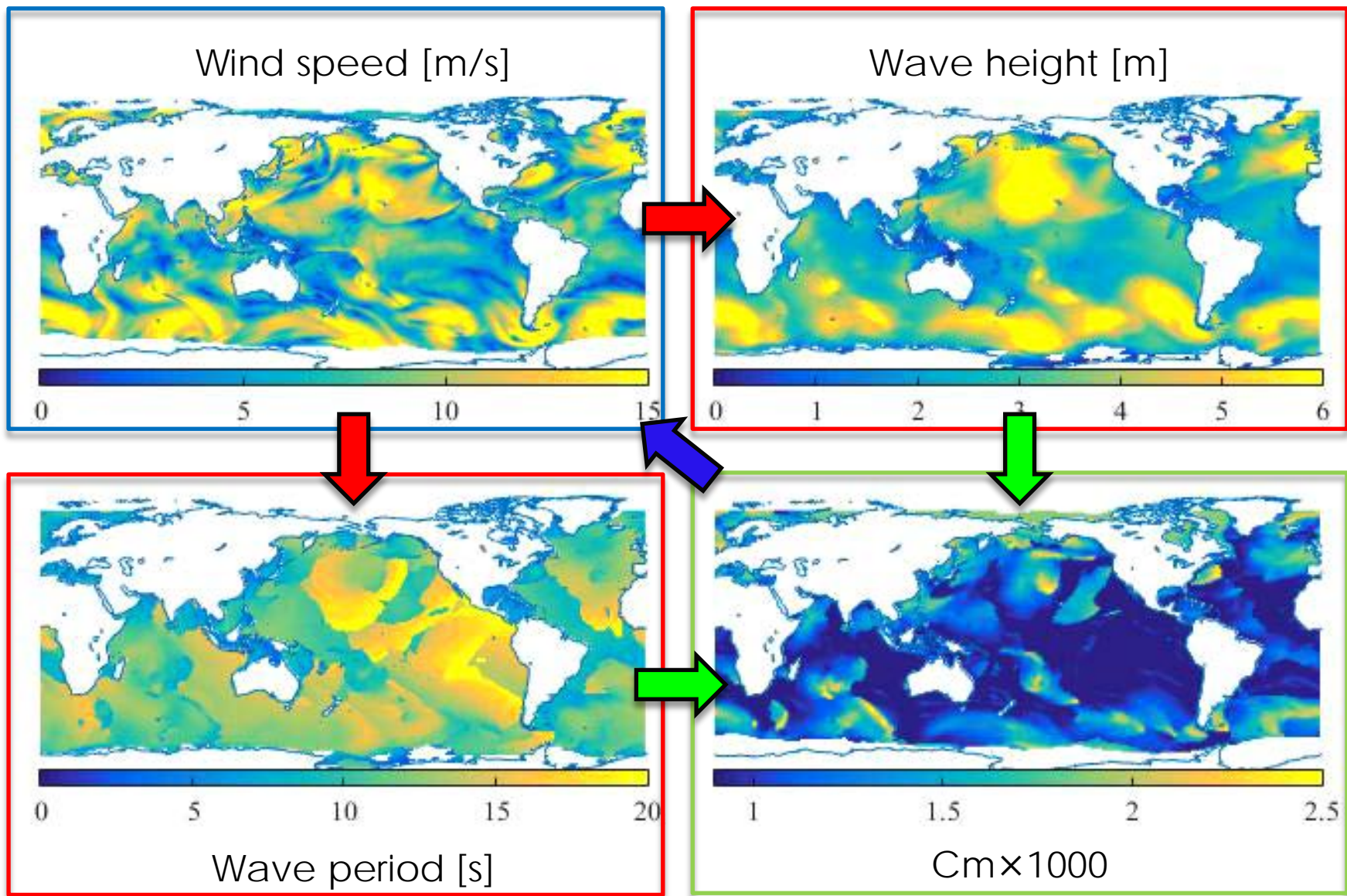
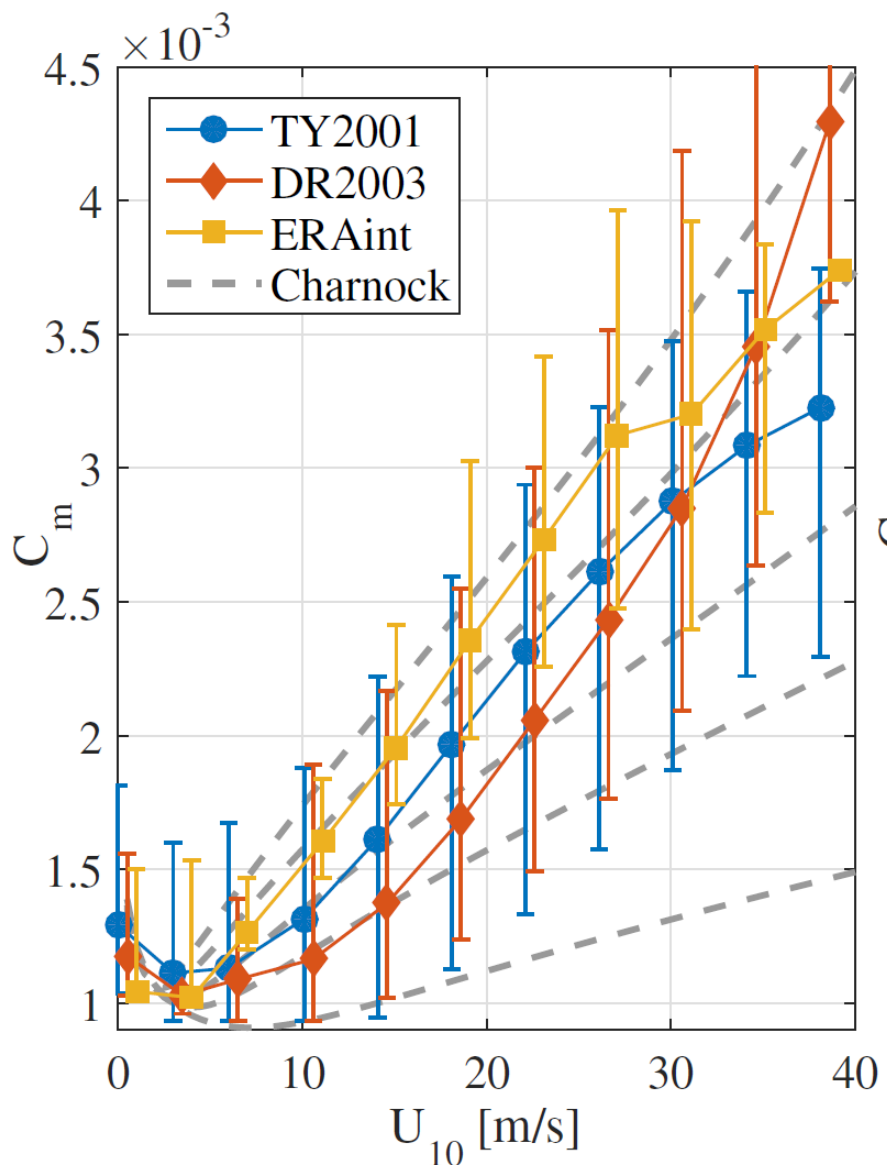
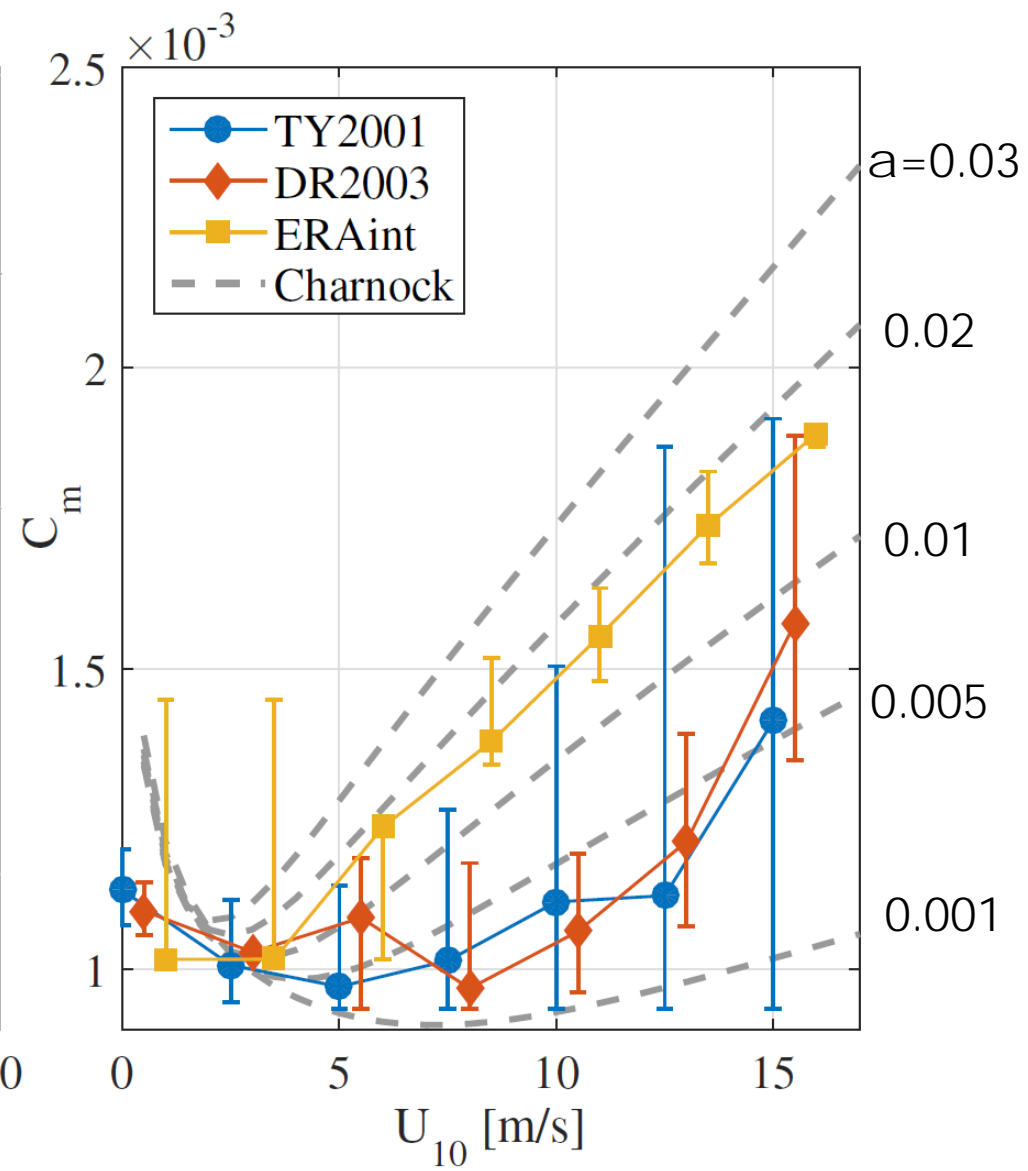


**Table 1.** Experiment description

Exp. name	Wave	Roughness	Time frame (Initial conditions)	Spatial resolution, GCM/WAVE
CHA0001		$\alpha = 0.001$		
CHA0005		$\alpha = 0.005$		
CHA001	No	$\alpha = 0.01$	1990-2014 (2)	$1.125^\circ / \text{—}$
CHA002		$\alpha = 0.02$ (default value)		
CHA003		$\alpha = 0.03$		
TY2001	Yes	Taylor and Yelland (2001)	1990-2014 (2)	$1.125^\circ / 1.25^\circ$
DR2003	Yes	Drennan et al. (2003)	1990-2014 (2)	$1.125^\circ / 1.125^\circ$



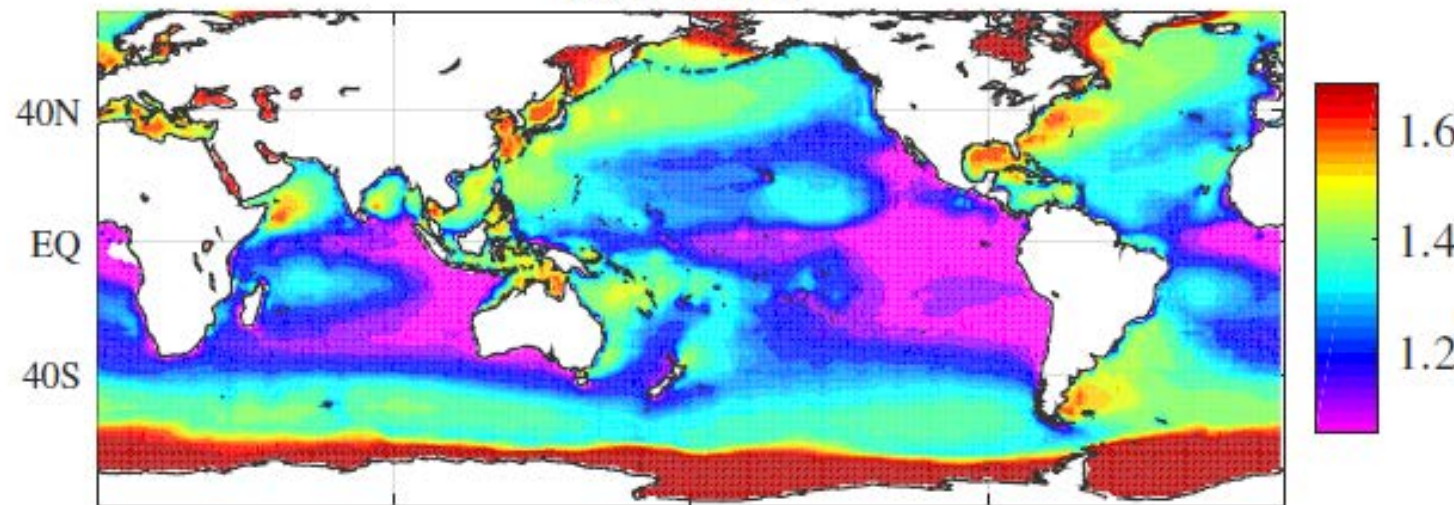
(a) Mid-high North Pacific



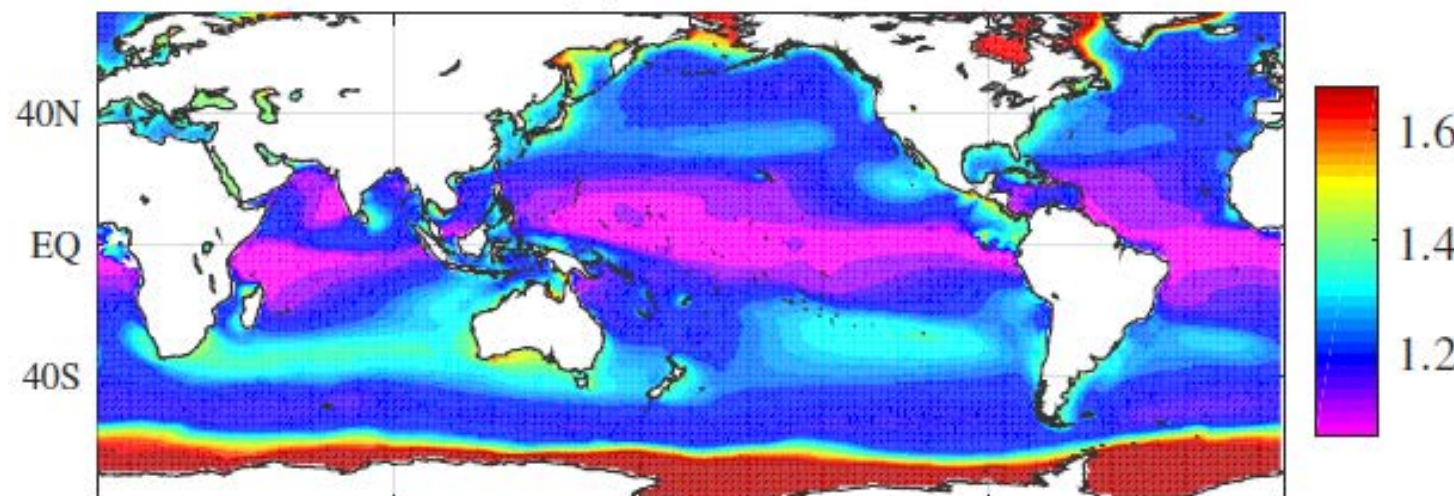
(b) Equatorial Pacific

# The spatial distribution of $C_m$ climatology (wind speeds: 10 m/s)

(a) TY2001

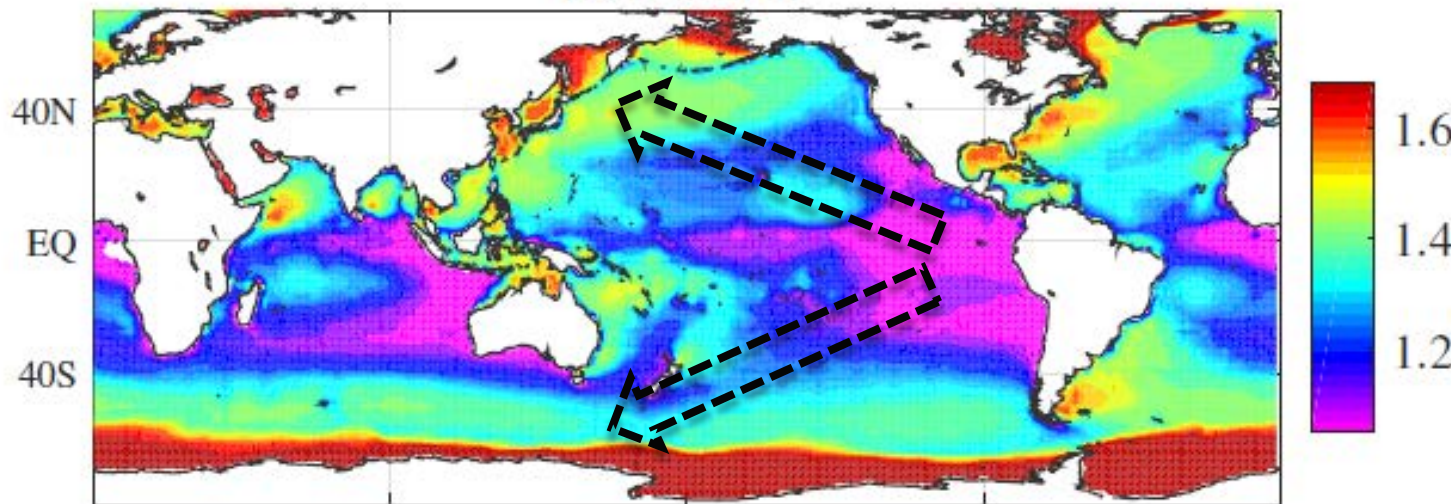


(b) DR2003

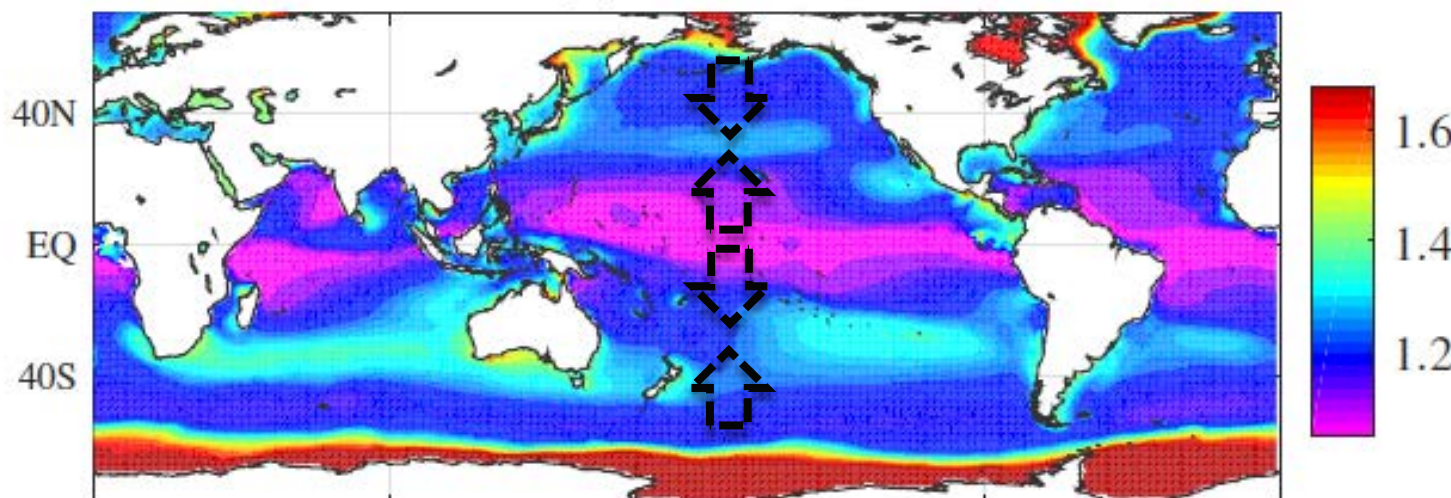


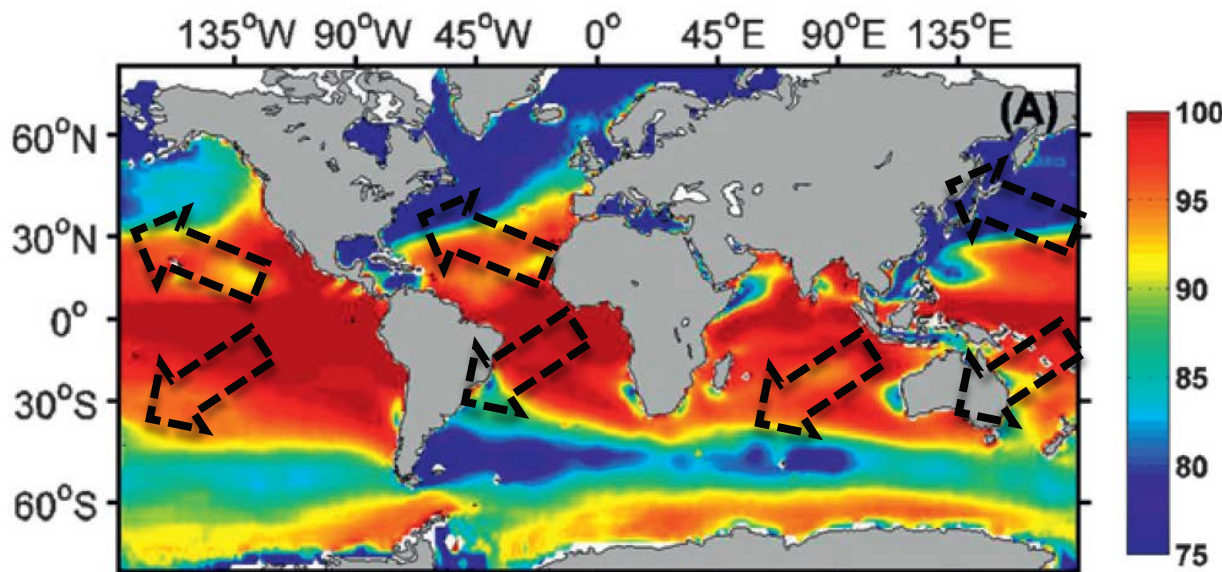
# The spatial distribution of $C_m$ climatology (wind speeds: 10 m/s)

(a) TY2001

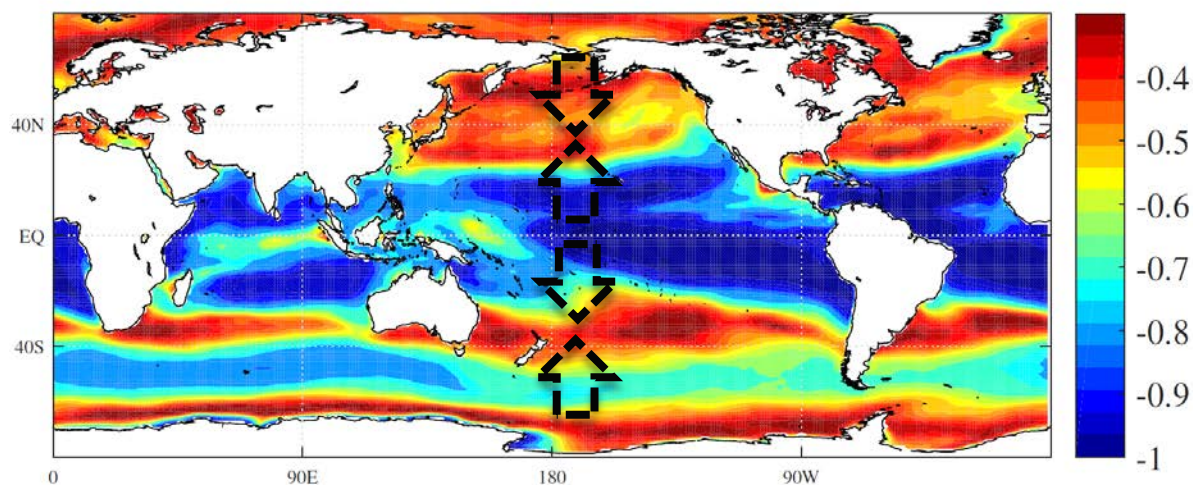


(b) DR2003





Swell probability  
Semedo et al.  
(2011, J.clim)

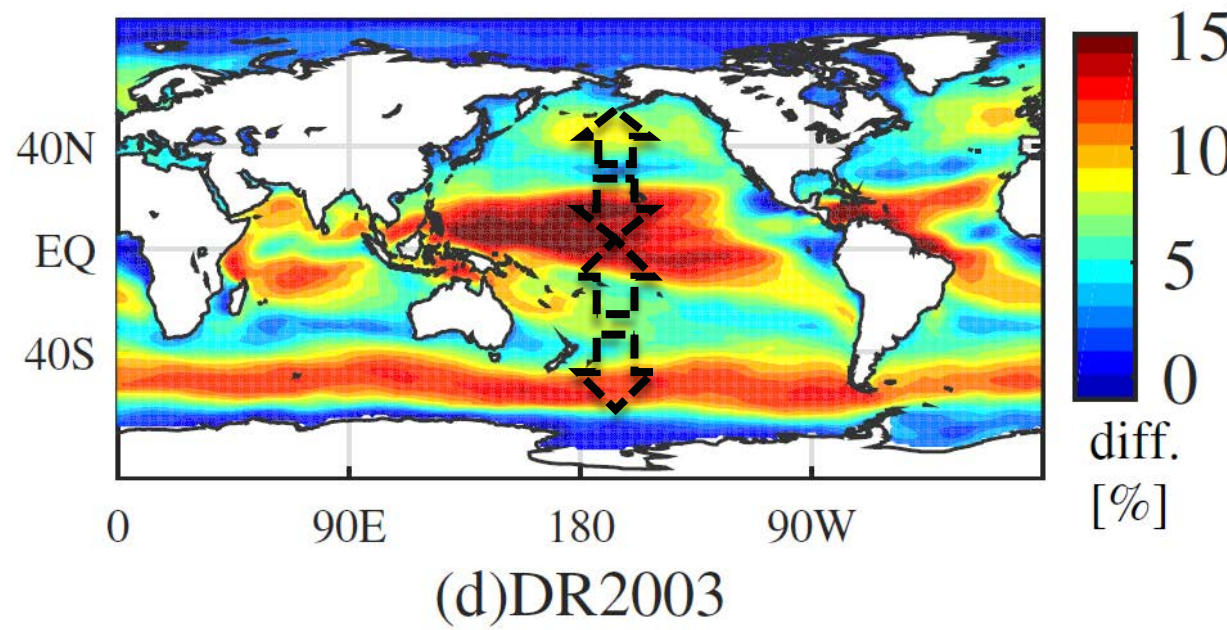
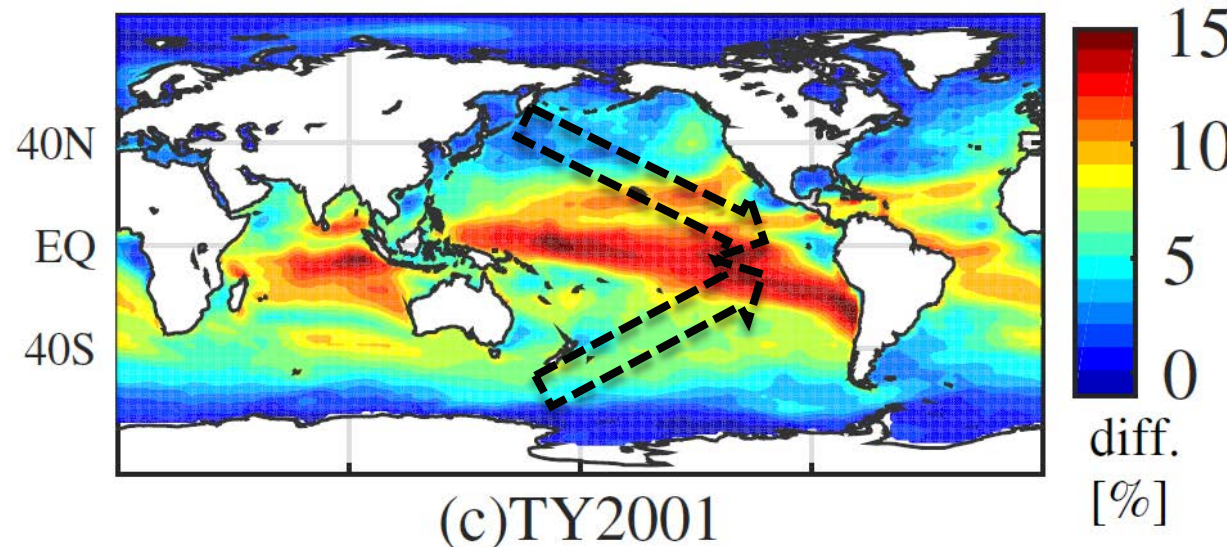


Wind direction  
stationarity

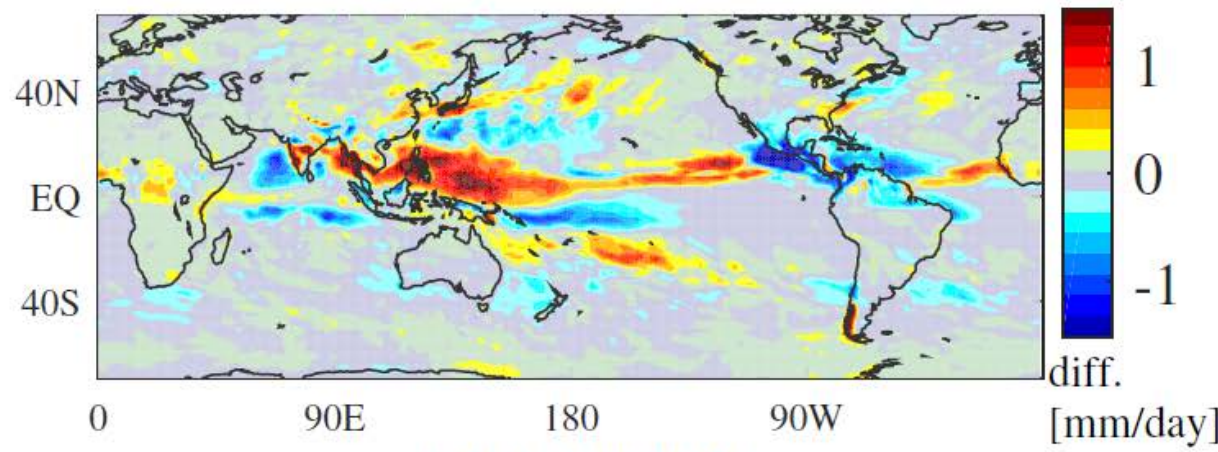
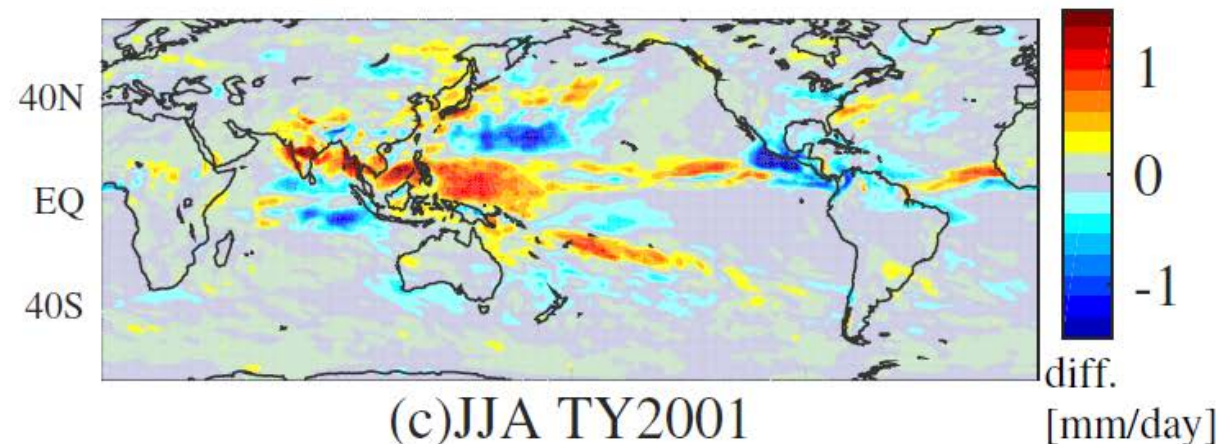
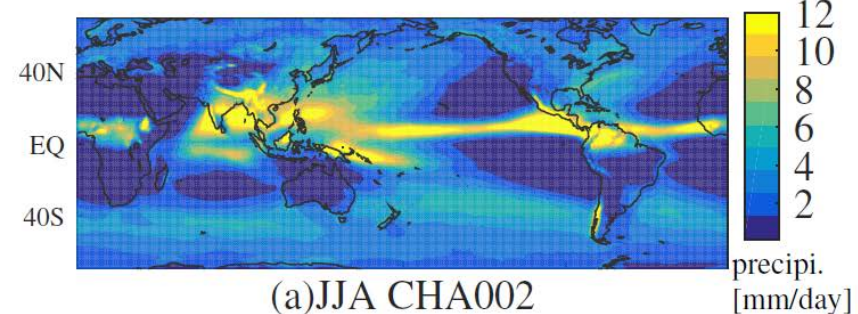
$$WDS_{ann} = \frac{1}{12} \sum_{month=1}^{12} \frac{\sqrt{\left(\sum_{n=1}^n u\right)^2 + \left(\sum_{n=1}^n v\right)^2}}{\sum_{n=1}^n \sqrt{u^2 + v^2}},$$

**Figure 12.** Wind direction stationarity ( $WDS_{ann}$ ). Note that the value is multiplied by -1.

# Sea surface wind speed climatology (diff. from CHA002)



# Precipitation climatology JJA



# Precipitation and Haley circulation (JJA)

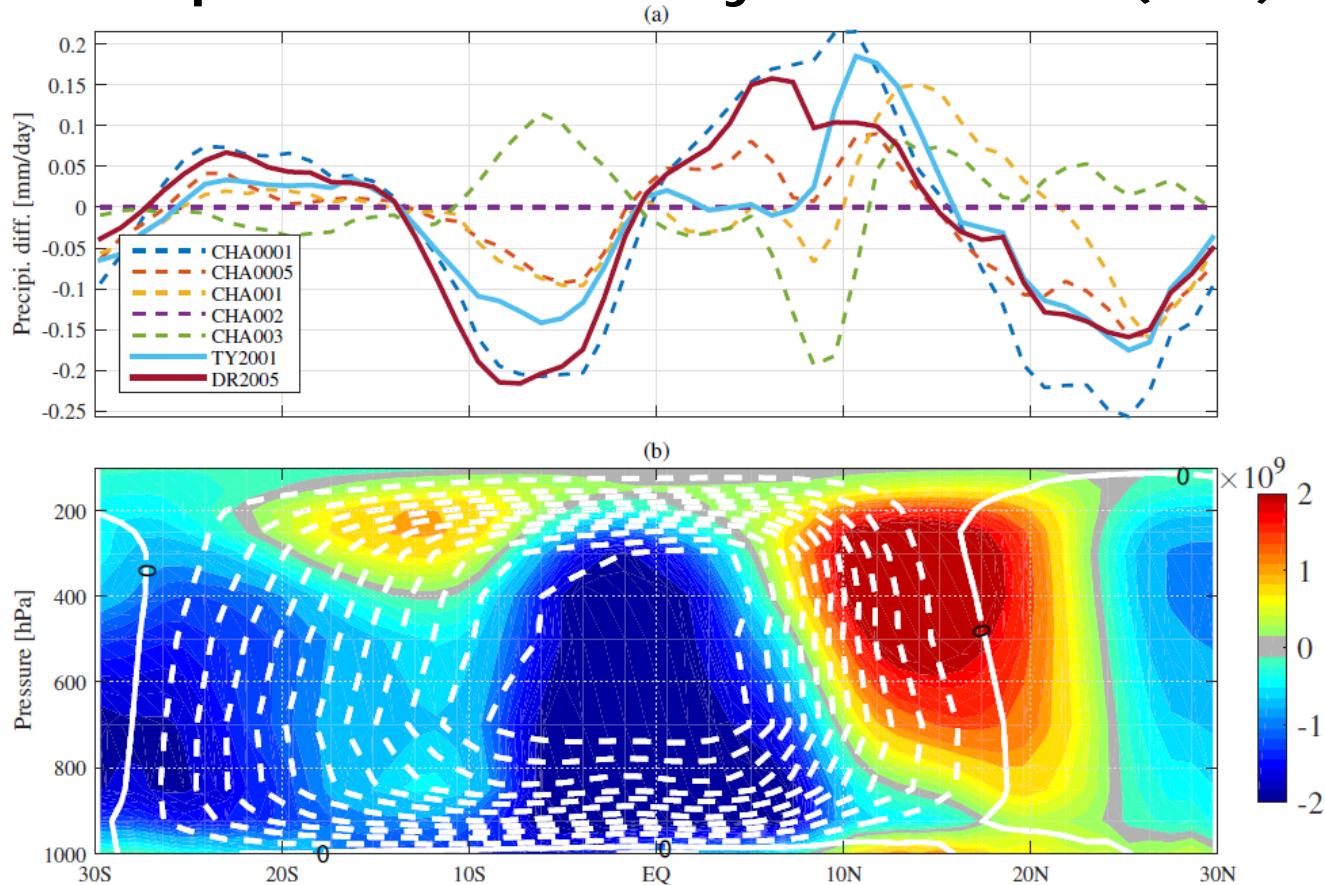


**Figure 8.** Panel (a): zonal mean precipitation climatology differences between all the experiments and CHA002 in JJA. Panel (b): Hadley circulation (mass stream functions) in JJA for CHA002 (white contour lines). Dashed contours indicate negative values, and solid contours indicate positive values. The contour interval is  $2 \times 10^{10}$  kg/s. The color shading shows the first EOF mode of the Hadley circulation among seven experiments indicating the representative difference among experiments.

EOF1  
Percent variance:  
87%

# Sea surface wind, precipitation and Haley circulation

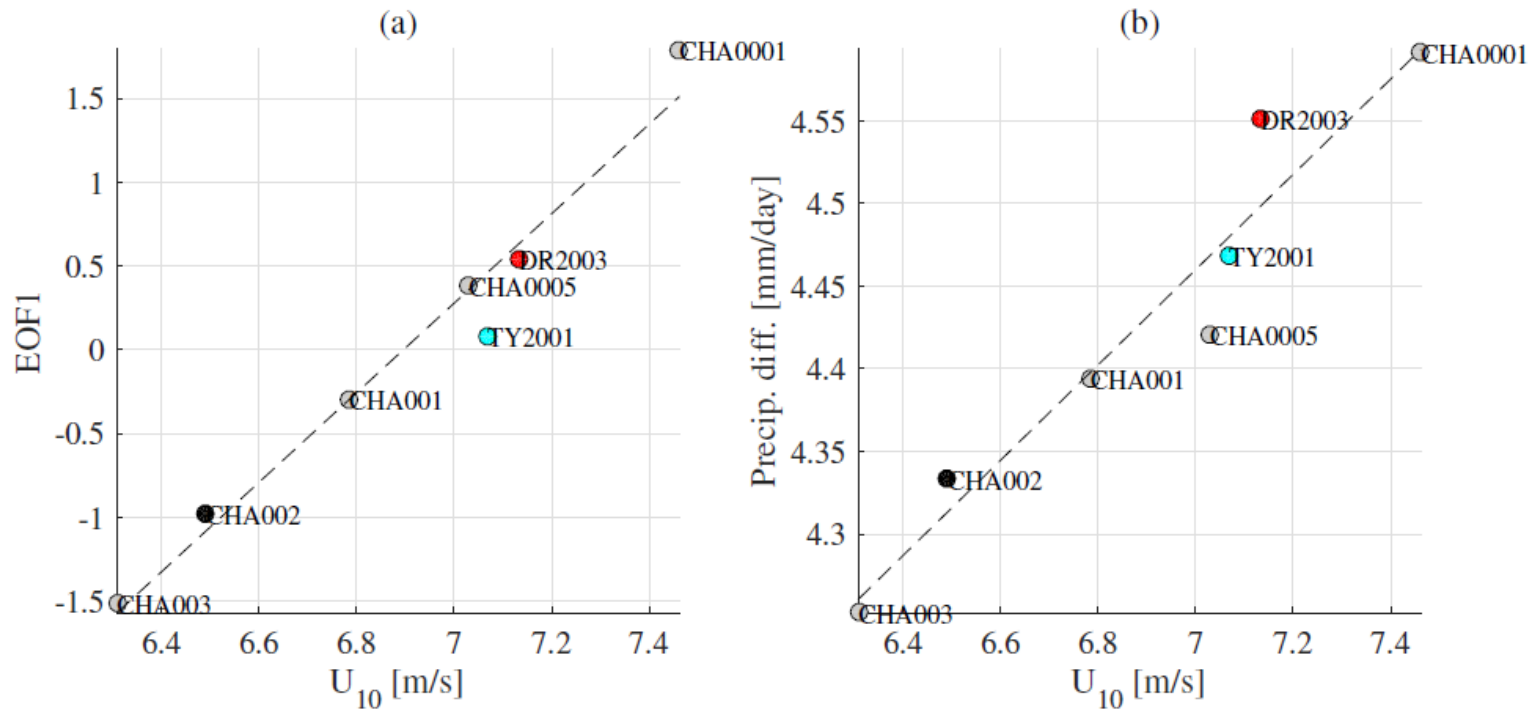


**Figure 9.** Panel (a): the relationship between  $U_{10}$  climatology at low latitudes and the Hadley circulation (represented by the coefficients of first EOF mode). Panel (b): the relationship between  $U_{10}$  climatology at low latitudes and the equatorial north-south differences in precipitation.

# Precipitation and Haley circulation (DJF)

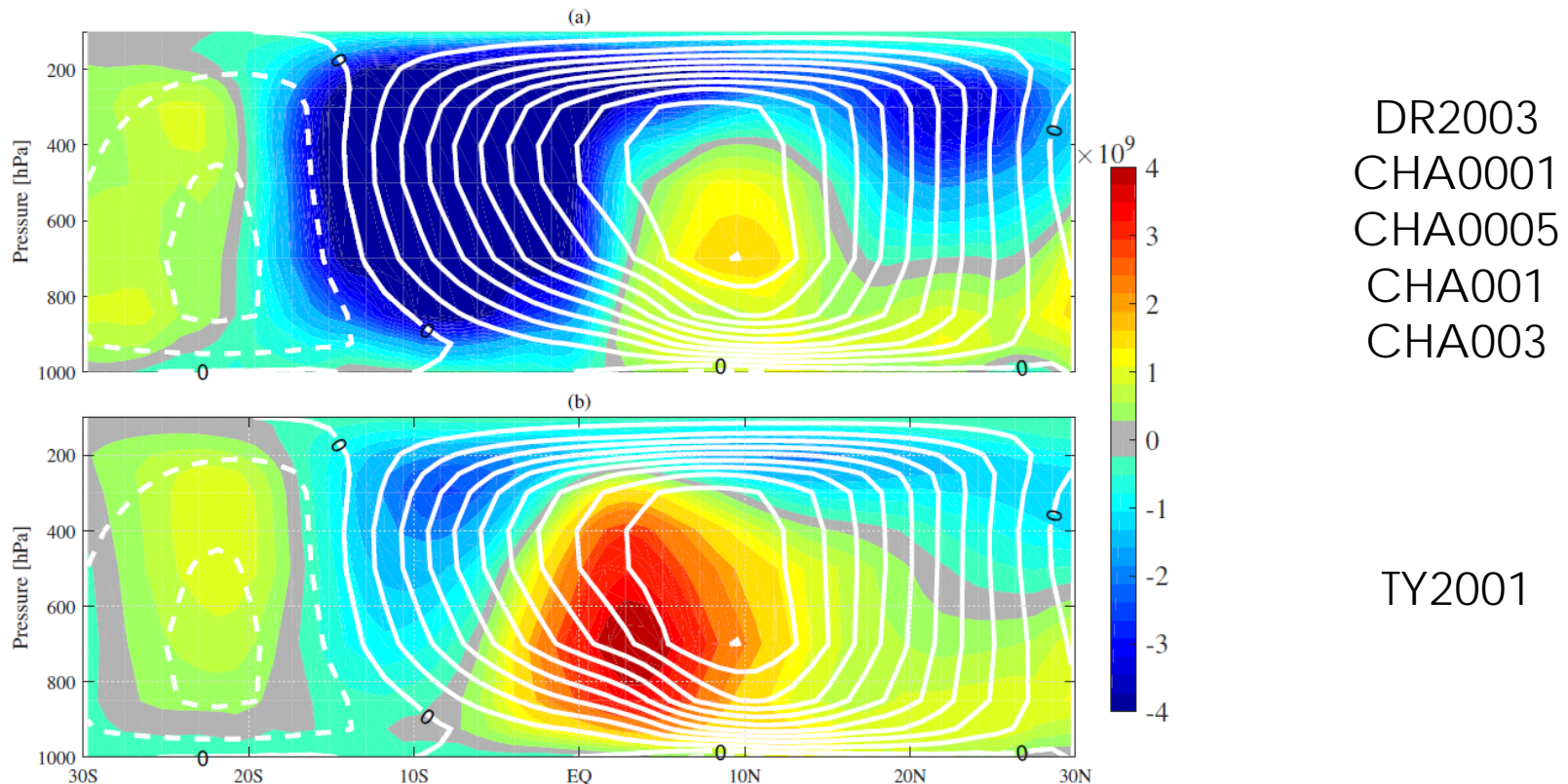


**Figure 11.** Panel (a): Hadley circulation (mass stream functions) in DJF for CHA002 (white contour lines).

Dashed contours indicate negative values, and solid contours indicate positive values. The contour interval is  $2 \times 10^{10}$  kg/s; the color shading shows the difference between CHA002 and TY2001. Panel (b): the first EOF mode of the Hadley circulation among the six experiments excluding TY2001; this is the same as

**Figure 8(b)**, but for DJF.

# Summary

- ❖ Global climate simulation using MRI-AGCM + WW3 coupled model (wave-dependent roughness)
- ❖ The spatial pattern of drag coefficient climatology
  - In wave steepness dependent roughness experiment
    - Swell dominance
  - Wave age dependent roughness experiment
    - wind direction stationarity
  - Wind climatology difference is 15% (lower latitudes)
- ❖ Impacts on precipitation (10~20%)
  - Hadley circulation
    - (JJA) The impacts of precipitation and Hadley circulation are similar between wave-coupled experiments and wind-dependent roughness experiment
    - (DJF) Impacts of wave steepness (swell) dependent roughness on atmospheric circulation is different when compared with wind or wave age (wind-sea) dependent roughness.

**end**

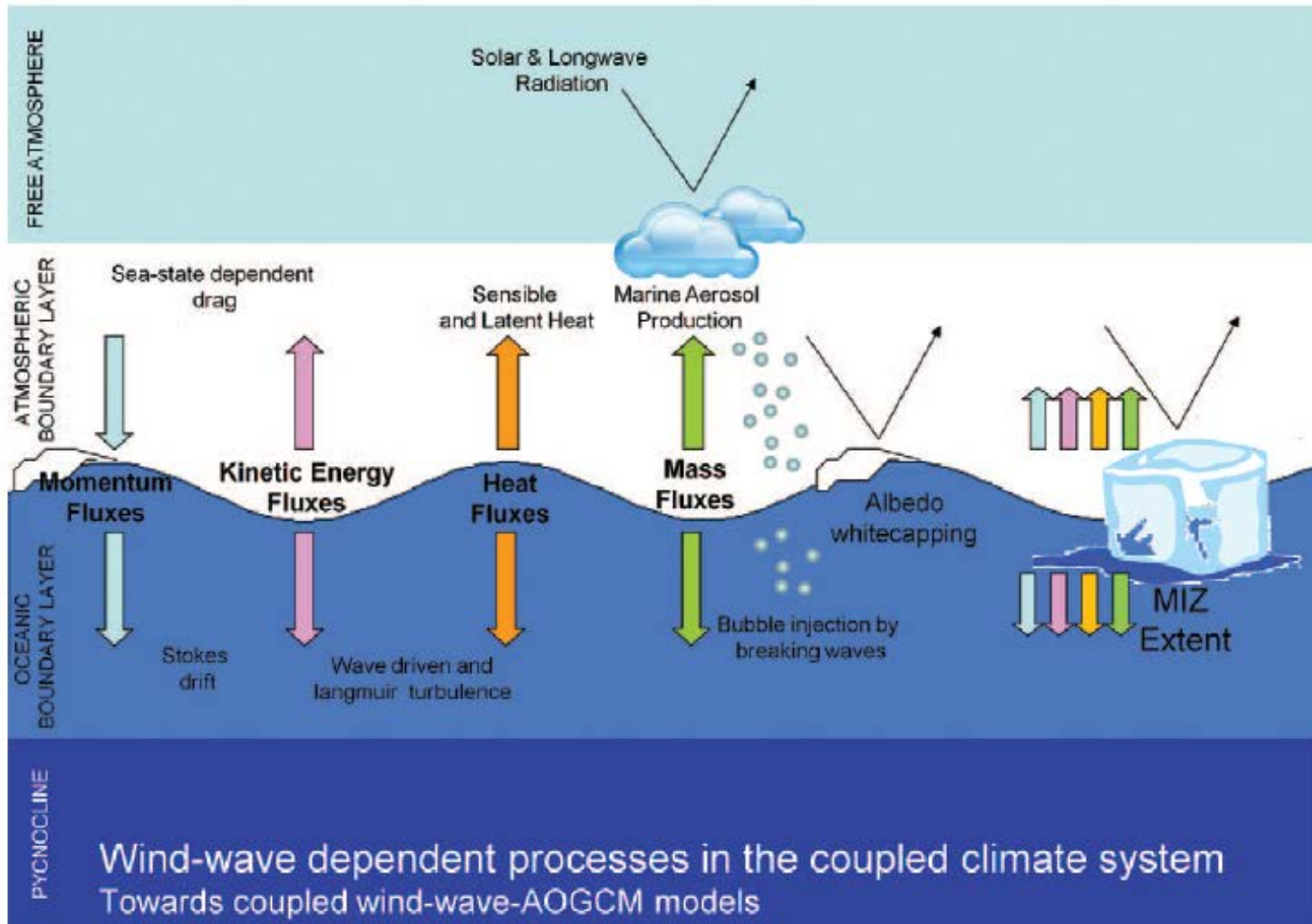


FIG. 1. A schematic view of the influence of waves on air-sea exchanges.

Cavalieri et al. (2012, BAMS)

# Ocean wave dependent momentum roughness length

**Wave steepness** dependent  
(Taylor and Yelland, 2001)

$$\frac{z_{0m}}{H_s} = A_1 \left( \frac{H_s}{L_p} \right)^{B_1}$$

$H_s$ : Significant wave height

$L_p$ : Peak wave length

$A_1=1200$ ,  $B_1=4.5$

- Toba3/2law

$$\frac{gH_s^{eq}}{u_*^2} = \alpha_t \left( \frac{gT_s^{eq}}{u_*} \right)^{3/2}$$

- Deviation from equilibrium

$$H_s = a_h H_s^{eq}$$

$$L_p = a_l L_p^{eq}$$

- Significant period -> peak

$$T_p^{eq} = C_t T_s^{eq}$$

- Deep water condition

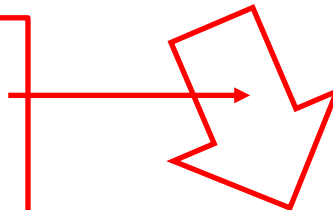
**Wave age** dependent  
(Drennan et al., 2003)

$$\frac{z_{0m}}{H_s} = A_2 \left( \frac{u_*}{c_p} \right)^{B_2}$$

$H_s$ : Significant wave height

$C_p$ : Wind-sea peak wave phase speed

$A_2=3.35$ ,  $B_2=3.4$



$$A_1 (2\pi)^{\frac{B_1+3}{2}} C_t^{\frac{3(B_1+1)}{2}} \alpha_t^{B_1+1} \frac{a_h^{B_1+1}}{a_l^{B_1}} \left( \frac{u_*}{c_p^{eq}} \right)^{\frac{B_1-3}{2}} \cdot \frac{u_*^2}{g}$$

$$= \alpha_{ty2001} \cdot \frac{u_*^2}{g}$$

$$z_{0m} = A_2 (2\pi)^{3/2} C_t^{3/2} \alpha_t a_h \left( \frac{u_*}{c_p} \right)^{B_2-3/2} \cdot \frac{u_*^2}{g}$$

$$= \alpha_{dr2003} \cdot \frac{u_*^2}{g}$$

$$\alpha_{ty2001} = 0.177 \frac{a_h^{5.5}}{a_l^{4.5}} \left( \frac{u_*}{c_p^{eq}} \right)^{0.75} \quad \alpha_{dr2003} = 3.029 a_h \left( \frac{u_*}{c_p^{eq}} \right)^{1.9}$$

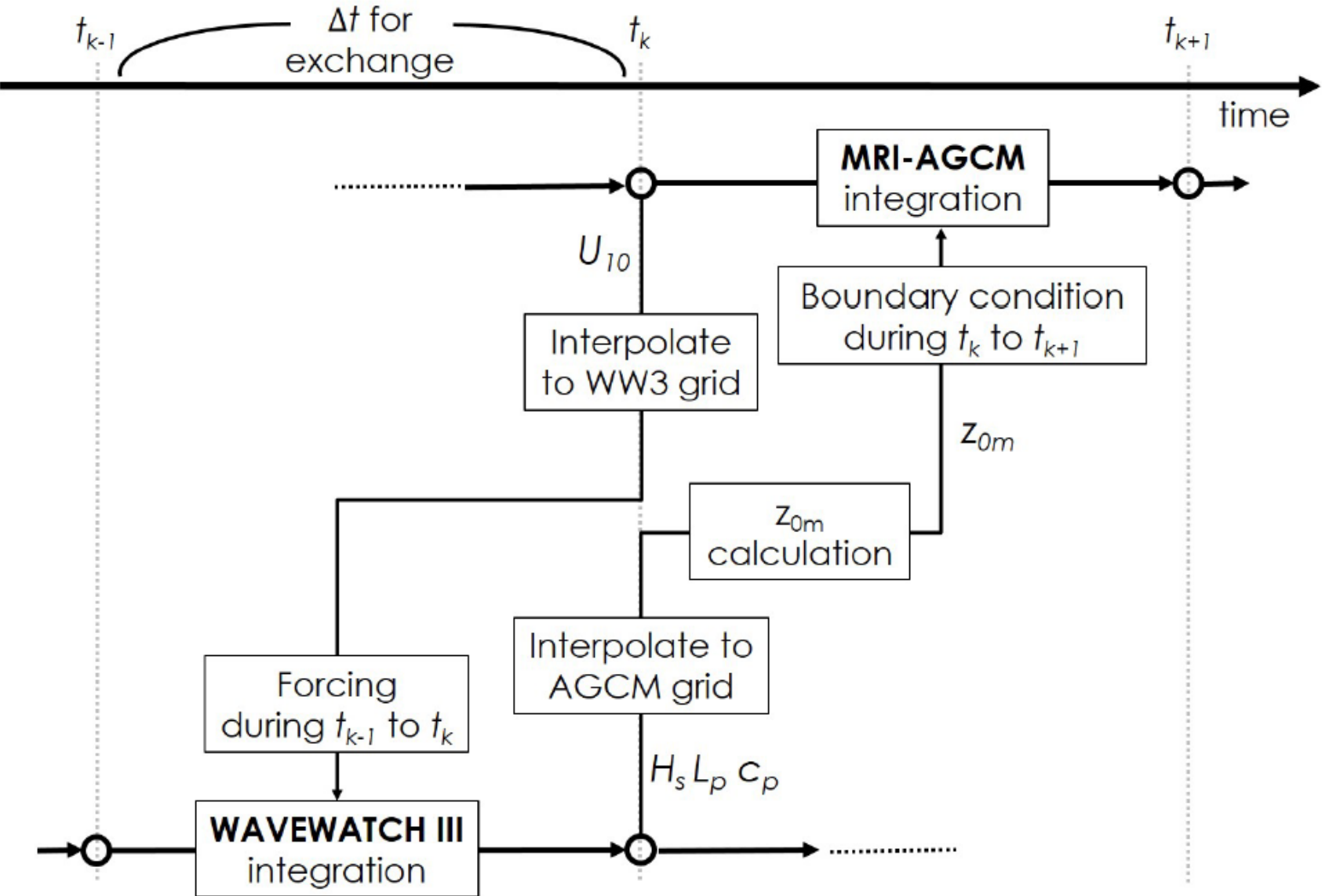
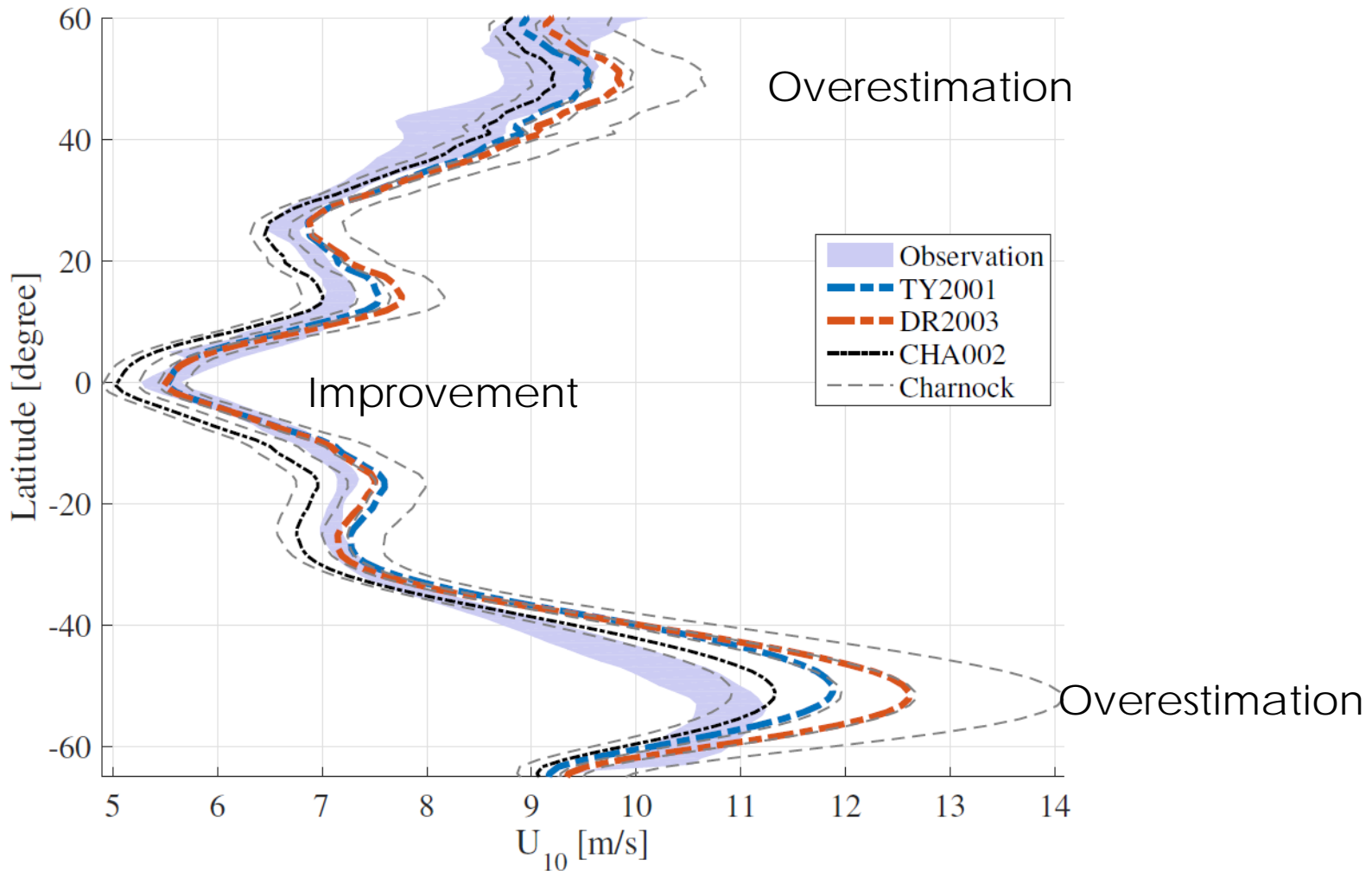


**Figure 1.** Schematic view of the coupling between MRI-AGCM and WAVEWATCH III.

# Sea surface wind speed climatology Comparison with satellite-based observations



Shimura et al. (2017)

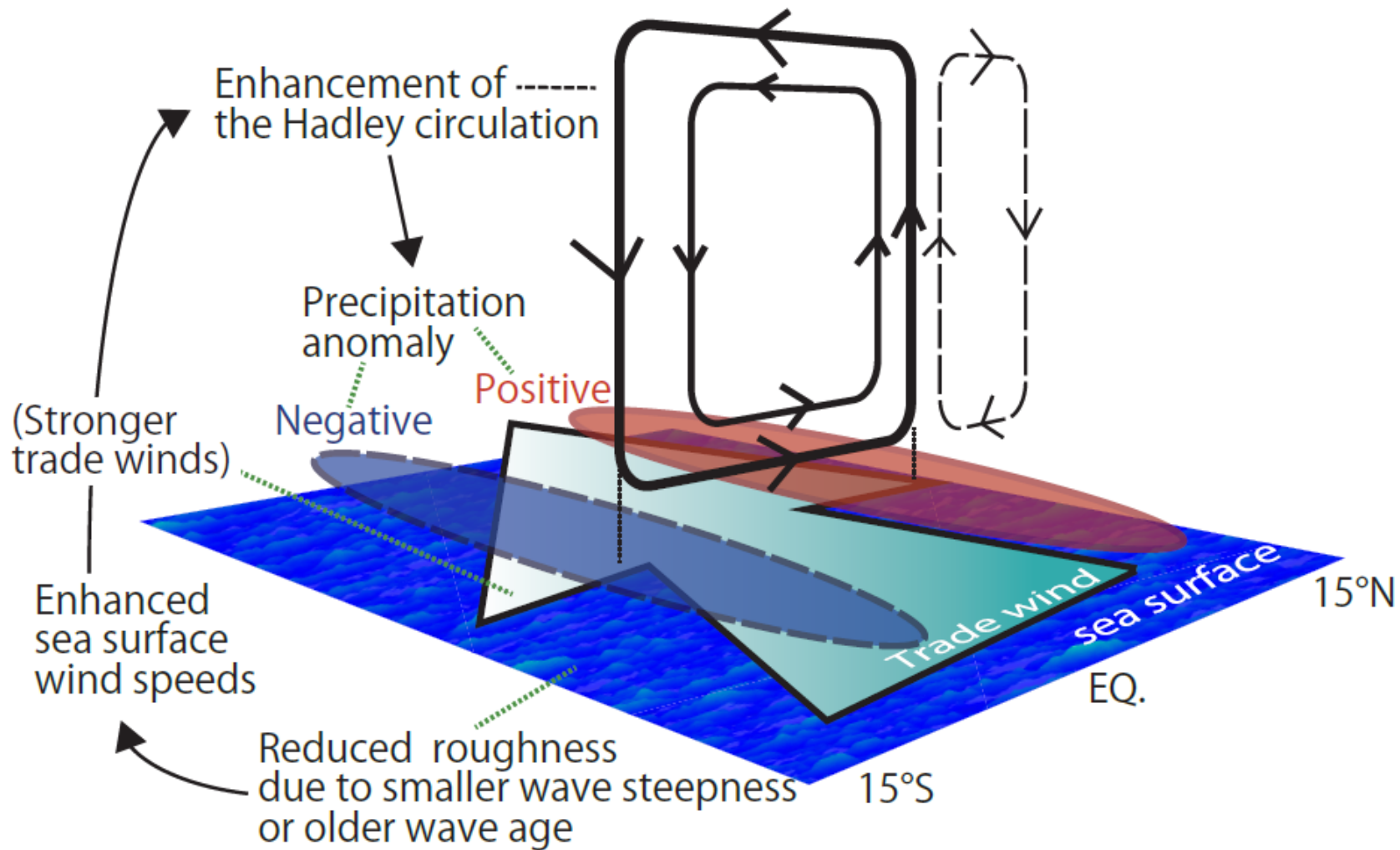


**Figure 10.** Overview of the atmospheric circulation responses to wave-dependent roughness in the boreal summer.